

Measuring the Astrophysical Galactic Plane Neutrino Flux and Searching for Galactic PeVatrons using the IceCube Multi-Flavor Astrophysical Neutrino Sample

The IceCube Collaboration

(a complete list of authors can be found at the end of the proceedings)

E-mail: thiesmeyer@icecube.wisc.edu, tyuan@icecube.wisc.edu,
lseen@icecube.wisc.edu, lu.lu@icecube.wisc.edu, karle@icecube.wisc.edu

Abstract: The IceCube Neutrino Observatory has provided new insights into the high-energy universe, in particular, unveiling neutrinos from the galactic plane. However, galactic neutrino sources are still unresolved. The recent detection of multi-PeV photons by LHAASO from the Cygnus region highlights its potential as a galactic neutrino source. Additionally, LHAASO, HAWC, and HESS have reported over forty galactic gamma-ray sources with energies above 100 TeV. Detecting neutrinos correlated with high-energy gamma-ray sources would provide compelling evidence of cosmic-ray acceleration in these galactic sources. In this work, we compile a 12.3-year, full-sky, all-flavor dataset, the IceCube Multi-Flavor Astrophysics Neutrino sample (ICEMAN). ICEMAN is the combination of three largely independent neutrino samples of different event morphologies and builds upon the previous work of the DNN-based cascade sample, Enhanced Starting Track Event Selection, and the Northern Track sample. Recent improvements in ice modeling and detector calibration are also incorporated into the cascade reconstruction. In addition to revisiting the galactic plane, we adopt two different analysis methods to search for galactic PeVatrons. First, we use a template-based approach to probe the Cygnus Cocoon region. Second, we use a point source hypothesis to find correlations between IceCube neutrinos and gamma-ray sources detected at energies greater than 100 TeV.

Corresponding authors:

Matthias Thiesmeyer^{1*}, Tianlu Yuan¹, Leo Seen¹, Lu Lu¹, Albrecht Karle¹

¹ *Dept. of Physics and Wisconsin IceCube Particle Astrophysics Center, University of Wisconsin—Madison*

* Presenter

39th International Cosmic Ray Conference (ICRC2025)
15–24 July 2025
Geneva, Switzerland



1. Introduction

The IceCube Neutrino Observatory is a cubic-kilometer neutrino detector located at the geographic south pole. In over ten years of operation time, IceCube has found evidence of multiple neutrino point sources, including the galaxy NGC 1068 [1] and the blazar TXS 0606+056 [2]. Both of these sources have been identified using *track*-like signatures in the detector, coming from charged current muon neutrino interactions from the North.

Charged-current interactions of electron and tau neutrinos, as well as neutral-current interactions of all flavors can take the morphology of *cascade*-like events in the detector. Reconstructed neutrinos from these interaction channels have been successfully used to observe the galactic plane as a neutrino source at 4.5σ significance [3]. Several other galactic plane analyses have been performed with different detection channels by IceCube [4][5] and the ANTARES neutrino detector [6], yielding only mildly significant detections of the galactic plane.

In this analysis, we report a combined fit utilizing starting muon tracks, cascades, and through-going muon tracks from the north, which are combined into a single dataset—the IceCube Multi-Flavor Astrophysical Neutrino Sample (ICEMAN). We use ICEMAN to provide an updated measurement of the galactic plane as a neutrino source, with an expected median local significance of 5.5σ .

2. Dataset

Three different event selections are combined to obtain an all-flavor, all-sky, combined dataset. The three different selections consist of cascades, starting tracks, and through-going tracks. Cascade

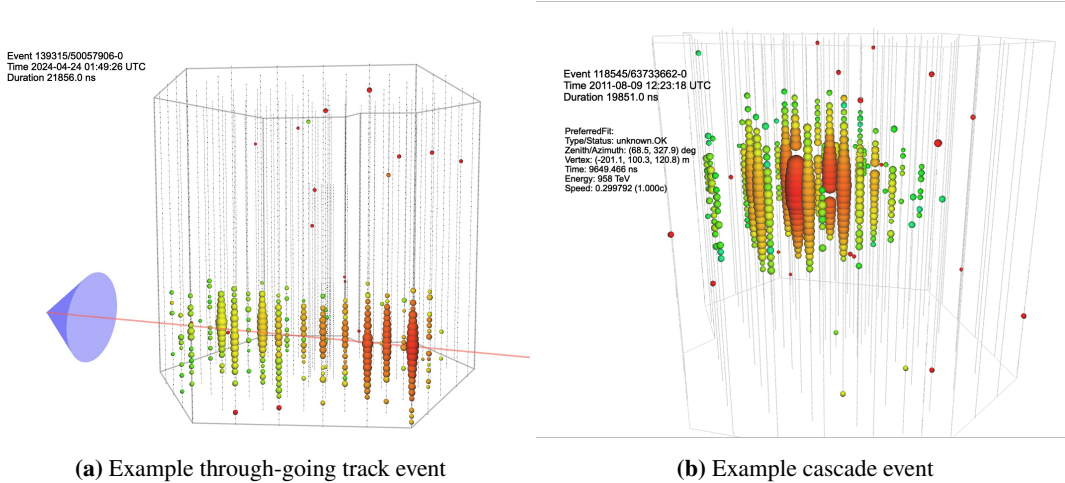


Figure 1: Two event views showing the two main topologies used in this analysis. A through-going track event (a) and a cascade event (b).

events are produced from neutral-current neutrino interactions of all flavors and charged-current interactions from electron and tau neutrinos. Due to their different morphology they can be more easily distinguished from track-like muons. This allows the rejection of the dominant background of atmospheric muons in the south. Therefore, this event selection does not rely on Earth absorption

for background rejection and is applicable to the whole sky. Compared to track-like events, they have worse angular resolution but better energy resolution. At 10 TeV, cascades have a median angular resolution of approximately 10° compared to about 0.5° for through-going tracks. However, their median energy uncertainty at 10 TeV is 3%, which is significantly better than the about 80% median energy resolution of through-going tracks. The cascade dataset used in this analysis uses a deep neural network (DNN) in the selection of cascade-like events, and is referred to as DNN cascades (DNNC). Various improvements [7] have been made to this dataset since the previous iteration [3]. The new version of this dataset now includes 85,199 events detected between the 13th of May, 2011 to the 28th of November, 2023.

Through-going tracks from the north, Northern Tracks (NT), are mainly produced by charged-current interactions of muon neutrinos. Because the interaction vertex can be outside the detector, the effective area is very large. To filter out atmospheric muons via Earth absorption, only neutrino candidates with zenith angles above 85 degrees, i.e, a bit more than half the sky, are selected. This leads to over 99.8% neutrino purity, i.e, a very low contamination of muons. The muon tracks induced from neutrino interactions have better angular resolution but a worse energy reconstruction compared to cascades. The dataset contains 13 years of IceCube data from the first of June, 2010 to the 28th of November, 2023. It has been used before in other IceCube point-source analyses [8].

The third subset consists of starting muon tracks. It is commonly referred to as the enhanced starting track event selection (ESTES). Like the through-going tracks from the north, these events are induced by charged current interactions of muon neutrinos. However, for starting tracks, the interaction vertex is inside the detector. This leads to a significant reduction of the atmospheric muon background, allowing for a full-sky application as well, at the cost of a smaller effective area. At 10 TeV, this data set has a median angular uncertainty of about one degree and a median energy uncertainty of about 30%. The dataset contains data from the 13th of May 2011 to the 28th of November 2023. It contains a total of 11,755 events. A version of this dataset with 10 years of livetime has been used in previous IceCube publications [4].

The per-flavor effective areas of the ICEMAN dataset are shown in Figure 2. In the combined sample, overlaps between the three different datasets are removed. The biggest set of overlaps is between ESTES and NT. These overlapping events are kept in the starting track set to maximize sensitivity. Figure 3 shows the exact number of overlaps.

3. Method

This is a template-based analysis where templates based on four different galactic emission models are being tested. The Fermi π^0 template [9], the KRA_γ^5 and KRA_γ^{50} templates [10] and the CRINGE template [11] with an unresolved sources component [12]. The results of this analysis will include the measurement of the model normalization for each of the four model hypotheses, the rejection of the null hypothesis under each model assumption, and the rejection of the global null hypothesis by the most significant model hypothesis after trial correction. We use an unbinned maximum likelihood method that utilizes the reconstructed direction, energy, and angular uncertainty of each neutrino candidate in the ICEMAN dataset.

The signal considered is the excess of neutrinos along the galactic plane over the only declination-dependent background fluxes of atmospheric muons, atmospheric neutrinos, and diffuse

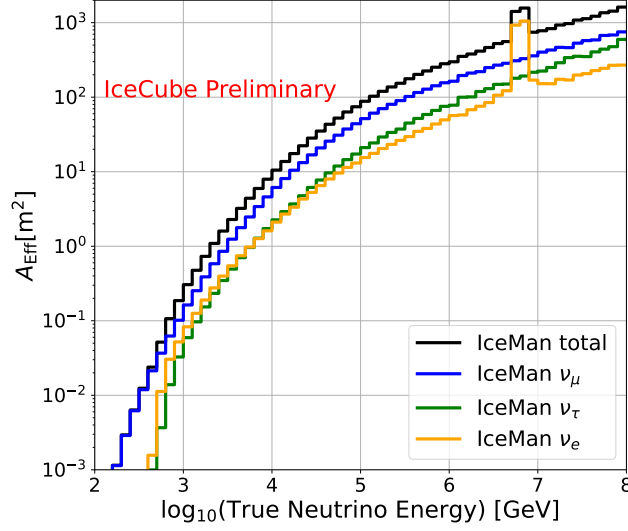


Figure 2: Per-flavor all-sky effective area in the ICEMAN sample.

astrophysical neutrinos.

To parameterize this excess prediction based on each model, templates of their respective prediction are folded with the effective area of each dataset. After normalizing, this creates a spatial probability density function (PDF) for each dataset and template combination. To account for the respective angular uncertainty of each event, each spatial PDF is smeared with a set of 2D Gaussian kernels corresponding to different angular uncertainties. They are then evaluated based on the uncertainty of the respective event. Figure 4 shows an example of the unsmeared PDF as well as an example of the smeared PDF for each sub-dataset.

To build the energy PDF, the MC is weighted with a single power law with a spectral index of -2.7 is used for the Fermi π^0 template. For the other three templates, the sky-averaged spectrum predicted by each template is used. The weighted MC is then binned in reconstructed energy. This way an energy PDF in reconstructed energy based on the predicted energy spectra is obtained. All nominal all-sky fluxes are shown in Figure 5.

To parameterize the declination-dependent backgrounds, a PDF of the density of neutrinos per declination is used. Since this background PDF is derived from data that contains partial contamination from the signal, a signal subtraction method is applied. The observed PDF from data \bar{D} , is characterized as the sum of the true isotropic background B , and the average density of the signal per declination band $\bar{S}(\delta_i)$:

$$\bar{D}(\delta_i, E_i) = \frac{n_s}{N} \bar{S}(\delta_i, E_i) + (1 - \frac{n_s}{N}) B(\delta_i, E_i). \quad (1)$$

Using this, the likelihood of observing n_s neutrinos is defined as shown in equation 2:

$$\mathcal{L}(n_s) = \prod_{i=1}^N \frac{n_s}{N} S(\delta_i, \alpha_i, E_i, \sigma_i) + \bar{D}_i(\sin(\delta_i), E_i) - \frac{n_s}{N} \bar{S}_i(\sin(\delta_i), E_i). \quad (2)$$

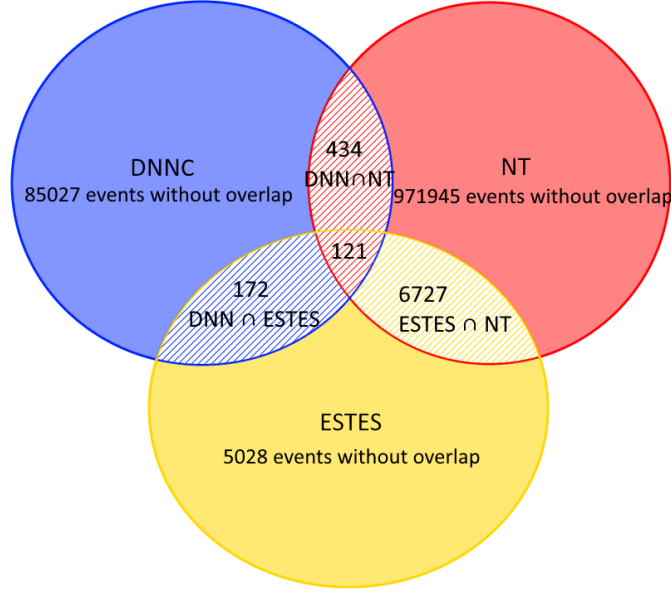


Figure 3: Sketch showing which dataset overlapping events are kept in. The event numbers exclusive to the datasets and in all overlapping zones are shown. The colors of the shaded regions show which dataset the overlap will stay in.

Then, the test statistic (TS) is defined as the likelihood ratio of fitting n_s neutrinos over zero neutrinos,

$$\text{TS} = 2 \ln \left[\frac{\mathcal{L}(\hat{n}_s)}{\mathcal{L}(n_s = 0)} \right]. \quad (3)$$

Using this method, we can derive the sensitivity and discovery potential of this analysis using pseudo-experiments. Here, a number of Monte-Carlo events corresponding to an injected flux are

Quantity	Fermi π^0 [10^{-12} TeV cm $^{-2}$ s $^{-1}$]	KRA $^5_\gamma$	KRA $^{50}_\gamma$	CRINGE
Sensitivity	4.68	0.13	0.10	0.13
Discovery Potential	18.7	0.49	0.40	0.53

Table 1: Sensitivity and discovery potentials for different models. For Fermi π^0 , the per-flavor flux at 100 TeV is reported. For the other three models, sensitivity and discovery potential are reported in units of model flux.

sampled from the spatial and energy distribution predicted by a chosen model. Data, with the right ascension coordinate randomized, is added to these signal events to account for the isotropic backgrounds. Table 1 shows the necessary flux for 50% of pseudo experiments to exceed the TS corresponding to a 5σ discovery for the four different templates. Since the flux measured in [3] is above the flux necessary to reach the 5σ threshold for the Fermi π^0 model, a 5σ pre-trial significance is a likely outcome of this analysis. In a set of pseudo-experiments, injecting the best fit flux of the previous measurement, we obtain a median local significance of 5.5σ for the Fermi π^0 model, as shown in Table 2.

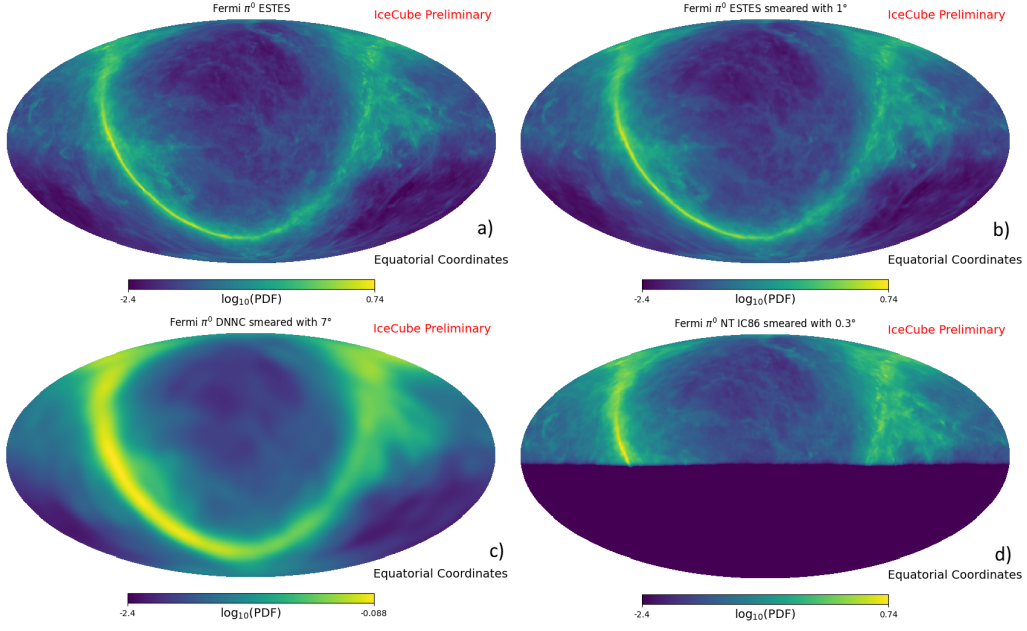


Figure 4: Spatial signal PDF for the Fermi π^0 template. Shown in a) acceptance weighted with ESTES without smearing. In b) acceptance weighted with ESTES and smeared with a Gaussian kernel of 0.3 degrees width. In c) the template is acceptance weighted with DNN Cascades and smeared with a Gaussian kernel of 7 degrees width. In d) the template is acceptance weighted with the Northern Tracks and smeared with a Gaussian of 0.3 degree width. These smearing widths are chosen based on the median angular uncertainty of the signal events in the respective datasets.

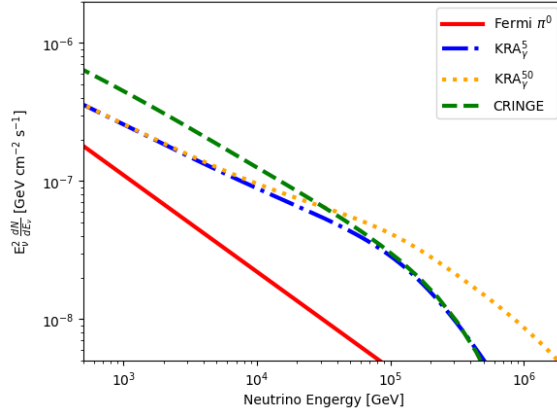


Figure 5: Nominal per-flavor flux prediction for all four templates used in this analysis.

4. Conclusion

In this work, three different sub-datasets in IceCube have been combined into a single multi-flavor all-sky dataset. We have detailed the improvements and dataset combination methods. Furthermore, we have shown the measurement technique with a combined likelihood in space and energy. Finally, we have calculated the sensitivities and discovery potentials under all four different model hypotheses. When compared to the values from the previous analysis [3] the sensitivities

Template	Fermi π^0	KRA $_{\gamma}^5$	KRA $_{\gamma}^{50}$	CRINGE
Median Significance (injecting Fermi π^0)	5.5σ	4.71σ	4.46σ	5.28σ

Table 2: Expected local significance from injecting the best fit model and flux of the previous analysis.

have improved by over 20%. These improvements highlight the capabilities of the combined ICEMAN dataset to make an improved measurement of the galactic plane as an extended neutrino source. Future IceCube analyses will utilize the ICEMAN dataset to measure the neutrino flux from the Cygnus region as an extended source and search for galactic neutrino sources based on a multi-messenger informed catalog [7].

References

- [1] **IceCube** Collaboration, *Science* **378** no. 6619, (2022) 538–543.
- [2] **IceCube** Collaboration, *Science* **361** no. 6398, (2018) 147–151.
- [3] **IceCube** Collaboration, *Science* **380** no. 6652, (2023) 1338–1343.
- [4] **IceCube** Collaboration, R. Abbasi *et al.*, “Time-integrated southern-sky neutrino source searches with 10 years of icecube starting-track events at energies down to 1 tev,” 2025. <https://arxiv.org/abs/2501.16440>.
- [5] P. M. Fuerst *et al.*, *PoS ICRC2023* (2023) 1046.
- [6] A. Albert *et al.*, *Physics Letters B* **841** (2023) 137951.
- [7] **IceCube** Collaboration, L. Seen, T. Yuan, L. Lu, M. Thiesmeyer, and A. Karle, *PoS ICRC2025* (these proceedings) 1169.
- [8] **IceCube** Collaboration, C. Bellenghi, M. H. Minh, T. Kontrimas, E. Manao, R. Ørsøe, and M. Wolf, *PoS ICRC2023* (2023) 1060.
- [9] M. Ackermann *et al.*, *The Astrophysical Journal* **750** no. 1, (Apr, 2012) 3.
- [10] D. Gaggero, D. Grasso, A. Marinelli, A. Urbano, and M. Valli, *The Astrophysical Journal* **815** no. 2, (Dec., 2015) L25.
- [11] G. Schwefer, P. Mertsch, and C. Wiebusch, *The Astrophysical Journal* **949** no. 1, (May, 2023) 16.
- [12] V. Vecchiotti, F. Zuccarini, F. L. Villante, and G. Pagliaroli, *The Astrophysical Journal* **928** no. 1, (Mar, 2022) 19.

Full Author List: IceCube Collaboration

R. Abbasi¹⁶, M. Ackermann⁶³, J. Adams¹⁷, S. K. Agarwalla^{39, a}, J. A. Aguilar¹⁰, M. Ahlers²¹, J.M. Alameddine²², S. Ali³⁵, N. M. Amin⁴³, K. Andeen⁴¹, C. Argüelles¹³, Y. Ashida⁵², S. Athanasiadou⁶³, S. N. Axani⁴³, R. Babu²³, X. Bai⁴⁹, J. Baines-Holmes³⁹, A. Balagopal V.^{39, 43}, S. W. Barwick²⁹, S. Bash²⁶, V. Basu⁵², R. Bay⁶, J. J. Beatty^{19, 20}, J. Becker Tjus^{9, b}, P. Behrens¹, J. Beise⁶¹, C. Bellenghi²⁶, B. Benkel⁶³, S. BenZvi⁵¹, D. Berley¹⁸, E. Bernardini^{47, c}, D. Z. Besson³⁵, E. Blaufuss¹⁸, L. Bloom⁵⁸, S. Blot⁶³, I. Bodo³⁹, F. Bontempo³⁰, J. Y. Book Motzkin¹³, C. Boscolo Meneguolo^{47, c}, S. Böser⁴⁰, O. Botner⁶¹, J. Böttcher¹, J. Braun³⁹, B. Brinson⁴, Z. Brisson-Tsouvoussis³², R. T. Burley², D. Butterfield³⁹, M. A. Campana⁴⁸, K. Carloni¹³, J. Carpio^{33, 34}, S. Chattopadhyay^{39, a}, N. Chau¹⁰, Z. Chen⁵⁵, D. Chirkin³⁹, S. Choi⁵², B. A. Clark¹⁸, A. Coleman⁶¹, P. Coleman¹, G. H. Collin¹⁴, D. A. Coloma Borja⁴⁷, A. Connolly^{19, 20}, J. M. Conrad¹⁴, R. Corley⁵², D. F. Cowen^{59, 60}, C. De Clercq¹¹, J. J. DeLaunay⁵⁹, D. Delgado¹³, T. Delmeulle¹⁰, S. Deng¹, P. Desiati³⁹, K. D. de Vries¹¹, G. de Wasseige³⁶, T. DeYoung²³, J. C. Díaz-Vélez³⁹, S. DiKerby²³, M. Dittmer⁴², A. Domi²⁵, L. Draper⁵², L. Dueser¹, D. Durnford²⁴, K. Dutta⁴⁰, M. A. DuVernois³⁹, T. Ehrhardt⁴⁰, L. Eidenschink²⁶, A. Eimer²⁵, P. Eller²⁶, E. Ellinger⁶², D. Elsässer²², R. Engel^{30, 31}, H. Erpenbeck³⁹, W. Esmail¹³, J. Evans¹⁸, P. A. Evenson⁴³, K. L. Fan¹⁸, K. Fang³⁹, K. Farrag¹⁵, A. R. Fazely⁵, A. Fedynitch⁵⁷, N. Feigl⁸, C. Finley⁵⁴, L. Fischer⁶³, D. Fox⁵⁹, A. Franckowiak⁹, S. Fukami⁶³, P. Fürst¹, J. Gallagher³⁸, E. Ganster¹, A. Garcia¹³, M. Garcia⁴³, G. Garg^{39, a}, E. Genton^{13, 36}, L. Gerhardt⁷, A. Ghadimi⁵⁸, C. Glaser⁶¹, T. Glüsenskamp⁶¹, J. G. Gonzalez⁴³, S. Goswami^{33, 34}, A. Granados²³, D. Grant¹², S. J. Gray¹⁸, S. Griffin³⁹, S. Griswold⁵¹, K. M. Groth²¹, D. Guevel³⁹, C. Günther¹, P. Gutjahr²², C. Ha⁵³, C. Haack²⁵, A. Hallgren⁶¹, L. Halve¹, F. Halzen³⁹, L. Hamacher¹, M. Ha Minh²⁶, M. Handt¹, K. Hanson³⁹, J. Hardin¹⁴, A. A. Harnisch²³, P. Hatch³², A. Haungs³⁰, J. Häußler¹, K. Helbing⁶², J. Hellrung⁹, B. Henke²³, L. Hennig²⁵, F. Henningsen¹², L. Heuermann¹, R. Hewett¹⁷, N. Heyer⁶¹, S. Hickford⁶², A. Hidvegi⁵⁴, C. Hill¹⁵, G. C. Hill², R. Hmaid¹⁵, K. D. Hoffman¹⁸, D. Hooper³⁹, S. Hori³⁹, K. Hoshina^{39, d}, M. Hostert¹³, W. Hou³⁰, T. Huber³⁰, K. Hultqvist⁵⁴, K. Hymon^{22, 57}, A. Ishihara¹⁵, W. Iwakiri¹⁵, M. Jacquart²¹, S. Jain³⁹, O. Janik²⁵, M. Jansson³⁶, M. Jeong⁵², M. Jin¹³, N. Kamp¹³, D. Kang³⁰, W. Kang⁴⁸, X. Kang⁴⁸, A. Kappes⁴², L. Kardum²², T. Karg⁶³, M. Karl²⁶, A. Karle³⁹, A. Katil²⁴, M. Kauer³⁹, J. L. Kelley³⁹, M. Khanal⁵², A. Khatee Zathul³⁹, A. Kheirandish^{33, 34}, H. Kimku⁵³, J. Kiryluk⁵⁵, C. Klein²⁵, S. R. Klein^{6, 7}, Y. Kobayashi¹⁵, A. Kochocki²³, R. Koirala⁴³, H. Kolanoski⁸, T. Kontrimas²⁶, L. Köpke⁴⁰, C. Kopper²⁵, D. J. Koskinen²¹, P. Koundal⁴³, M. Kowalski^{8, 63}, T. Kozynets²¹, N. Krieger⁹, J. Krishnamoorthi^{39, a}, T. Krishnan¹³, K. Kruiswijk³⁶, E. Krupczak²³, A. Kumar⁶³, E. Kun⁹, N. Kurahashi⁴⁸, N. Lad⁶³, C. Lagunas Gualda²⁶, L. Lallement Arnaud¹⁰, M. Lamoureux³⁶, M. J. Larson¹⁸, F. Lauber⁶², J. P. Lazar³⁶, K. Leonard DeHoltan⁶⁰, A. Leszczyńska⁴³, J. Liao⁴, C. Lin⁴³, Y. T. Liu⁶⁰, M. Liubarska²⁴, C. Love⁴⁸, L. Lu³⁹, F. Lucarelli²⁷, W. Luszczyk^{19, 20}, Y. Lyu^{6, 7}, J. Madsen³⁹, E. Magnus¹¹, K. B. M. Mahn²³, Y. Makino³⁹, E. Manao²⁶, S. Mancina^{47, e}, A. Mand³⁹, I. C. Mariş¹⁰, S. Marka⁴⁵, Z. Marka⁴⁵, L. Marten¹, I. Martinez-Soler¹³, R. Maruyama⁴⁴, J. Mauro³⁶, F. Mayhew²³, F. McNally³⁷, J. V. Mead²¹, K. Meagher³⁹, S. Mechbal⁶³, A. Medina²⁰, M. Meier¹⁵, Y. Merckx¹¹, L. Merten⁹, J. Mitchell⁵, L. Molchany⁴⁹, T. Montaruli²⁷, R. W. Moore²⁴, Y. Morii¹⁵, A. Mosbrugger²⁵, M. Moulai³⁹, D. Mousadi⁶³, E. Moyaux³⁶, T. Mukherjee³⁰, R. Naab⁶³, M. Nakos³⁹, U. Naumann⁶², J. Necker⁶³, L. Neste⁵⁴, M. Neumann⁴², H. Niederhausen²³, M. U. Nisa²³, K. Noda¹⁵, A. Noell¹, A. Novikov⁴³, A. Obertacke Pollmann¹⁵, V. O'Dell³⁹, A. Olivas¹⁸, R. Orsoe²⁶, J. Osborn³⁹, E. O'Sullivan⁶¹, V. Palusova⁴⁰, H. Pandya⁴³, A. Parenti¹⁰, N. Park³², V. Parrish²³, E. N. Paudel⁵⁸, L. Paul⁴⁹, C. Pérez de los Heros⁶¹, T. Pernice⁶³, J. Peterson³⁹, M. Plum⁴⁹, A. Pontén⁶¹, V. Poojyam⁵⁸, Y. Popovych⁴⁰, M. Prado Rodriguez³⁹, B. Pries²³, R. Procter-Murphy¹⁸, G. T. Przybylski⁷, L. Pyras⁵², C. Raab³⁶, J. Rack-Helleis⁴⁰, N. Rad⁶³, M. Ravn⁶¹, K. Rawlins³, Z. Rechav³⁹, A. Rehman³⁹, I. Reistoffer⁴⁹, E. Resconi²⁶, S. Reusch⁶³, C. D. Rho⁵⁶, W. Rhode²², L. Ricca³⁶, B. Riedel³⁹, A. Rifaie⁶², E. J. Roberts², S. Robertson^{6, 7}, M. Rongen²⁵, A. Rosted¹⁵, C. Rott⁵², T. Ruhe²², L. Ruohan²⁶, D. Ryckbosch²⁸, J. Saffer³¹, D. Salazar-Gallegos²³, P. Sampathkumar³⁰, A. Sandrock⁶², G. Sanger-Johnson²³, M. Santander⁵⁸, S. Sarkar⁴⁶, J. Savelberg¹, M. Scarnera³⁶, P. Schaile²⁶, M. Schaufel¹, H. Schieler³⁰, S. Schindler²⁵, L. Schlickmann⁴⁰, B. Schlüter⁴², F. Schlüter¹⁰, N. Schmeisser⁶², T. Schmidt¹⁸, F. G. Schröder^{30, 43}, L. Schumacher²⁵, S. Schwirn¹, S. Sclafani¹⁸, D. Seckel⁴³, L. Seen³⁹, M. Seikh³⁵, S. Seunarine⁵⁰, P. A. Seyle Myhr³⁶, R. Shah⁴⁸, S. Shefali³¹, N. Shimizu¹⁵, B. Skrzypek⁶, R. Snihur³⁹, J. Soedingrekso²², A. Sjøgaard²¹, D. Soldin⁵², P. Soldin¹, G. Sommani⁹, C. Spannfellner²⁶, G. M. Spiczak⁵⁰, C. Spiering⁶³, J. Stachurska²⁸, M. Stamatikos²⁰, T. Stanev⁴³, T. Stezelberger⁷, T. Stürwald⁶², T. Stuttard²¹, G. W. Sullivan¹⁸, I. Taboada⁴, S. Ter-Antonyan⁵, A. Terliuk²⁶, A. Thakuri⁴⁹, M. Thiesmeyer³⁹, W. G. Thompson¹³, J. Thwaites³⁹, S. Tilav⁴³, K. Tollefson²³, S. Toscano¹⁰, D. Tosi³⁹, A. Trettin⁶³, A. K. Upadhyay^{39, a}, K. Upshaw⁵, A. Vaidyanathan⁴¹, N. Valtonen-Mattila^{9, 61}, J. Valverde⁴¹, J. Vandenbroucke³⁹, T. van Eeden⁶³, N. van Eijndhoven¹¹, L. van Rootselaar²², J. van Santen⁶³, F. J. Vara Carbonell⁴², F. Varsi³¹, M. Venugopal³⁰, M. Vereecken³⁶, S. Vergara Carrasco¹⁷, S. Verpoest⁴³, D. Veske⁴⁵, A. Vijai¹⁸, J. Villarreal¹⁴, C. Walck⁵⁴, A. Wang⁴, E. Warrick⁵⁸, C. Weaver²³, P. Weigel¹⁴, A. Weindl³⁰, J. Weldert⁴⁰, A. Y. Wen¹³, C. Wendt³⁹, J. Werthebach²², M. Weyrauch³⁰, N. Whitehorn²³, C. H. Wiebusch¹, D. R. Williams⁵⁸, L. Witthaus²², M. Wolf²⁶, G. Wrede²⁵, X. W. Xu⁵, J. P. Yañez²⁴, Y. Yao³⁹, E. Yildizci³⁹, S. Yoshida¹⁵, R. Young³⁵, F. Yu¹³, S. Yu⁵², T. Yuan³⁹, A. Zegarelli⁹, S. Zhang²³, Z. Zhang⁵⁵, P. Zhelnin¹³, P. Zilberman³⁹

¹ III. Physikalisches Institut, RWTH Aachen University, D-52056 Aachen, Germany² Department of Physics, University of Adelaide, Adelaide, 5005, Australia³ Dept. of Physics and Astronomy, University of Alaska Anchorage, 3211 Providence Dr., Anchorage, AK 99508, USA⁴ School of Physics and Center for Relativistic Astrophysics, Georgia Institute of Technology, Atlanta, GA 30332, USA⁵ Dept. of Physics, Southern University, Baton Rouge, LA 70813, USA⁶ Dept. of Physics, University of California, Berkeley, CA 94720, USA⁷ Lawrence Berkeley National Laboratory, Berkeley, CA 94720, USA⁸ Institut für Physik, Humboldt-Universität zu Berlin, D-12489 Berlin, Germany⁹ Fakultät für Physik & Astronomie, Ruhr-Universität Bochum, D-44780 Bochum, Germany¹⁰ Université Libre de Bruxelles, Science Faculty CP230, B-1050 Brussels, Belgium

- ¹¹ Vrije Universiteit Brussel (VUB), Dienst ELEM, B-1050 Brussels, Belgium
¹² Dept. of Physics, Simon Fraser University, Burnaby, BC V5A 1S6, Canada
¹³ Department of Physics and Laboratory for Particle Physics and Cosmology, Harvard University, Cambridge, MA 02138, USA
¹⁴ Dept. of Physics, Massachusetts Institute of Technology, Cambridge, MA 02139, USA
¹⁵ Dept. of Physics and The International Center for Hadron Astrophysics, Chiba University, Chiba 263-8522, Japan
¹⁶ Department of Physics, Loyola University Chicago, Chicago, IL 60660, USA
¹⁷ Dept. of Physics and Astronomy, University of Canterbury, Private Bag 4800, Christchurch, New Zealand
¹⁸ Dept. of Physics, University of Maryland, College Park, MD 20742, USA
¹⁹ Dept. of Astronomy, Ohio State University, Columbus, OH 43210, USA
²⁰ Dept. of Physics and Center for Cosmology and Astro-Particle Physics, Ohio State University, Columbus, OH 43210, USA
²¹ Niels Bohr Institute, University of Copenhagen, DK-2100 Copenhagen, Denmark
²² Dept. of Physics, TU Dortmund University, D-44221 Dortmund, Germany
²³ Dept. of Physics and Astronomy, Michigan State University, East Lansing, MI 48824, USA
²⁴ Dept. of Physics, University of Alberta, Edmonton, Alberta, T6G 2E1, Canada
²⁵ Erlangen Centre for Astroparticle Physics, Friedrich-Alexander-Universität Erlangen-Nürnberg, D-91058 Erlangen, Germany
²⁶ Physik-department, Technische Universität München, D-85748 Garching, Germany
²⁷ Département de physique nucléaire et corpusculaire, Université de Genève, CH-1211 Genève, Switzerland
²⁸ Dept. of Physics and Astronomy, University of Gent, B-9000 Gent, Belgium
²⁹ Dept. of Physics and Astronomy, University of California, Irvine, CA 92697, USA
³⁰ Karlsruhe Institute of Technology, Institute for Astroparticle Physics, D-76021 Karlsruhe, Germany
³¹ Karlsruhe Institute of Technology, Institute of Experimental Particle Physics, D-76021 Karlsruhe, Germany
³² Dept. of Physics, Engineering Physics, and Astronomy, Queen's University, Kingston, ON K7L 3N6, Canada
³³ Department of Physics & Astronomy, University of Nevada, Las Vegas, NV 89154, USA
³⁴ Nevada Center for Astrophysics, University of Nevada, Las Vegas, NV 89154, USA
³⁵ Dept. of Physics and Astronomy, University of Kansas, Lawrence, KS 66045, USA
³⁶ Centre for Cosmology, Particle Physics and Phenomenology - CP3, Université catholique de Louvain, Louvain-la-Neuve, Belgium
³⁷ Department of Physics, Mercer University, Macon, GA 31207-0001, USA
³⁸ Dept. of Astronomy, University of Wisconsin—Madison, Madison, WI 53706, USA
³⁹ Dept. of Physics and Wisconsin IceCube Particle Astrophysics Center, University of Wisconsin—Madison, Madison, WI 53706, USA
⁴⁰ Institute of Physics, University of Mainz, Staudinger Weg 7, D-55099 Mainz, Germany
⁴¹ Department of Physics, Marquette University, Milwaukee, WI 53201, USA
⁴² Institut für Kernphysik, Universität Münster, D-48149 Münster, Germany
⁴³ Bartol Research Institute and Dept. of Physics and Astronomy, University of Delaware, Newark, DE 19716, USA
⁴⁴ Dept. of Physics, Yale University, New Haven, CT 06520, USA
⁴⁵ Columbia Astrophysics and Nevis Laboratories, Columbia University, New York, NY 10027, USA
⁴⁶ Dept. of Physics, University of Oxford, Parks Road, Oxford OX1 3PU, United Kingdom
⁴⁷ Dipartimento di Fisica e Astronomia Galileo Galilei, Università Degli Studi di Padova, I-35122 Padova PD, Italy
⁴⁸ Dept. of Physics, Drexel University, 3141 Chestnut Street, Philadelphia, PA 19104, USA
⁴⁹ Physics Department, South Dakota School of Mines and Technology, Rapid City, SD 57701, USA
⁵⁰ Dept. of Physics, University of Wisconsin, River Falls, WI 54022, USA
⁵¹ Dept. of Physics and Astronomy, University of Rochester, Rochester, NY 14627, USA
⁵² Department of Physics and Astronomy, University of Utah, Salt Lake City, UT 84112, USA
⁵³ Dept. of Physics, Chung-Ang University, Seoul 06974, Republic of Korea
⁵⁴ Oskar Klein Centre and Dept. of Physics, Stockholm University, SE-10691 Stockholm, Sweden
⁵⁵ Dept. of Physics and Astronomy, Stony Brook University, Stony Brook, NY 11794-3800, USA
⁵⁶ Dept. of Physics, Sungkyunkwan University, Suwon 16419, Republic of Korea
⁵⁷ Institute of Physics, Academia Sinica, Taipei, 11529, Taiwan
⁵⁸ Dept. of Physics and Astronomy, University of Alabama, Tuscaloosa, AL 35487, USA
⁵⁹ Dept. of Astronomy and Astrophysics, Pennsylvania State University, University Park, PA 16802, USA
⁶⁰ Dept. of Physics, Pennsylvania State University, University Park, PA 16802, USA
⁶¹ Dept. of Physics and Astronomy, Uppsala University, Box 516, SE-75120 Uppsala, Sweden
⁶² Dept. of Physics, University of Wuppertal, D-42119 Wuppertal, Germany
⁶³ Deutsches Elektronen-Synchrotron DESY, Platanenallee 6, D-15738 Zeuthen, Germany
^a also at Institute of Physics, Sachivalaya Marg, Sainik School Post, Bhubaneswar 751005, India
^b also at Department of Space, Earth and Environment, Chalmers University of Technology, 412 96 Gothenburg, Sweden
^c also at INFN Padova, I-35131 Padova, Italy
^d also at Earthquake Research Institute, University of Tokyo, Bunkyo, Tokyo 113-0032, Japan
^e now at INFN Padova, I-35131 Padova, Italy

Acknowledgments

The authors gratefully acknowledge the support from the following agencies and institutions: USA – U.S. National Science Foundation-Office of Polar Programs, U.S. National Science Foundation-Physics Division, U.S. National Science Foundation-EPSCoR, U.S. National Science Foundation-Office of Advanced Cyberinfrastructure, Wisconsin Alumni Research Foundation, Center for High Throughput Computing (CHTC) at the University of Wisconsin–Madison, Open Science Grid (OSG), Partnership to Advance Throughput Computing (PATH), Advanced Cyberinfrastructure Coordination Ecosystem: Services & Support (ACCESS), Frontera and Ranch computing project at the Texas Advanced Computing Center, U.S. Department of Energy-National Energy Research Scientific Computing Center, Particle astrophysics research computing center at the University of Maryland, Institute for Cyber-Enabled Research at Michigan State University, Astroparticle physics computational facility at Marquette University, NVIDIA Corporation, and Google Cloud Platform; Belgium – Funds for Scientific Research (FRS-FNRS and FWO), FWO Odysseus and Big Science programmes, and Belgian Federal Science Policy Office (Belspo); Germany – Bundesministerium für Forschung, Technologie und Raumfahrt (BMFTR), Deutsche Forschungsgemeinschaft (DFG), Helmholtz Alliance for Astroparticle Physics (HAP), Initiative and Networking Fund of the Helmholtz Association, Deutsches Elektronen Synchrotron (DESY), and High Performance Computing cluster of the RWTH Aachen; Sweden – Swedish Research Council, Swedish Polar Research Secretariat, Swedish National Infrastructure for Computing (SNIC), and Knut and Alice Wallenberg Foundation; European Union – EGI Advanced Computing for research; Australia – Australian Research Council; Canada – Natural Sciences and Engineering Research Council of Canada, Calcul Québec, Compute Ontario, Canada Foundation for Innovation, WestGrid, and Digital Research Alliance of Canada; Denmark – Villum Fonden, Carlsberg Foundation, and European Commission; New Zealand – Marsden Fund; Japan – Japan Society for Promotion of Science (JSPS) and Institute for Global Prominent Research (IGPR) of Chiba University; Korea – National Research Foundation of Korea (NRF); Switzerland – Swiss National Science Foundation (SNSF).